Chemical Engineering Journal 108 (2005) 239–248

Chemical Engineering Journal

www.elsevier.com/locate/cej

Reaction pathways and product yields in mild thermal cracking of vacuum residues: A multi-lump kinetic model

Jasvinder Singh [a,*], M.M. Kumar [a], Alok K. Saxena [a,1], Surendra Kumar [b]

[a] *Indian Institute of Petroleum, Dehradun 248005, Uttaranchal, India*

[b] *Department of Chemical Engineering, Indian Institute of Technology Roorkee, Roorkee 247667, Uttaranchal, India*

Received 29 April 2004; received in revised form 15 February 2005; accepted 15 February 2005

Abstract

Mild thermal cracking of vacuum residue is used in an oil refinery for 'bottom of the barrel' upgradation in the form of visbreaking. Lab scale studies were conducted in a batch reactor to study the cracking behavior of vacuum residues at mild severity conditions in terms of lumping of distillate fractions. Four residual feedstocks of Indian and Middle East origin, being processed in Indian refineries were studied for five different residence times between 3 and 15 min and four different temperatures ranging between 400 and 430 °C. A five lumped and seven parameter kinetic model has been developed for the prediction of yield of products. The lumping scheme chosen was based on the most value added products, i.e., gas, gasoline, light gas oil (LGO) and vacuum gas oil (VGO). Delplot analysis has been used for determining reaction pathways.

Keywords: Visbreaking; Residues; Kinetics; Modelling; Thermal cracking

1. Introduction

The processing of heavy feedstocks/vacuum residues into light high value products has drawn the attention of refiners worldwide due to increasing demand of light oil fractions and depleting reserves of sweet crude oils. With the shrinking profit margins in refinery business, visbreaking has gained renewed interest due to being a low cost option for upgradation of heavy crudes and residual feedstocks. The definition of a heavy crude oil includes the long and short residues, i.e., "bottom of the barrel", conventional heavy crude oils having API lower than 20, tar sand, unconventional oil from enhanced oil recovery and some shale oils. A thermal cracking process is in general more attractive as compared to catalytic conversion process for processing heavy feeds because typical residual feedstocks contain a very high metal content which acts as poison for the catalyst, as well as other catalyst deactivating compounds, e.g., asphaltenes, resins, etc.

Although thermal cracking is quite old process, yet subject of kinetic modelling of thermal cracking of petroleum feed stocks did not get much attention initially. The reasons were complexity of reactions as well as non-availability of infrastructural facilities for the analysis and computations. A deeper understanding is mandatory for the efficient design and operation of industrial visbreaker. Some earlier attempts were made to explain the thermal cracking with simple description using a single first-order reaction [1–3]. Later attempts were made using more comprehensive reaction schemes using as much as 16 pseudo components. A critical appraisal of the significant work on kinetics and modelling studies reported in literature has been presented in the following subsection.

1.1. Reaction conditions and order of reaction

The studies on thermal cracking of the residual stocks have been reported for the temperature range of 400–530 °C and pressure range from atmospheric to 12 kg/cm^2 (g). The

* Corresponding author. Tel: +91 1352660204; Fax: +91 1352660202.
E-mail address: jsingh@iip.res.in (J. Singh).

[1] Present address: S.S. Consultants, Flat No. 207-28, Feroz Gandhi Marg, Lajpat Nagar III, New Delhi 110024, India.

1385-8947/$ – see front matter © 2005 Elsevier B.V. All rights reserved.
doi:10.1016/j.cej.2005.02.018

Nomenclature

Name of feedstocks

NGSR	North Gujarat short residue
BHSR	Bombay high short residue from BPCL
MVBF	Mathura refinery vis-breaker feed
HRA	Haldia refinery asphalt

Notations

E	activation energy (kJ/mol)
F_0	initial weight of feedstock (g)
F	weight of feedstock lump at time t
G	weight of gas lump at any time t
GLN	weight of gasoline lump at any time t
k	reaction rate constant (min^{-1})
LGO	weight of light gas oil lump at any time t
T	temperature (°C, K)
VGO	weight of vacuum gas oil lump at any time t
X	fractional conversion of feedstock
y_i	fractional yield of the ith lump

residence time varies between few minutes to 2 h; however, it depends upon the volume of the reactor as well as the type of operation (continuous or batch reactor, coil or soaker visbreaking). The feedstocks studied are long and short residues as well as separated asphaltenes from crude oils from different sources including synthetic crude from coal liquefaction.

Most of the studies reported first-order reaction kinetics for thermal cracking of the residual feedstocks. However, Martinez et al. [4] has presented second-order rate kinetics in their studies on thermal cracking of asphaltenes separated from coal liquefaction. According to them, second-order kinetics provides an excellent fit for the products obtained at 425–450 °C. However, the coke and oil + gas data deviate from predicted second-order behaviour, when the experimental conditions are more severe (reaction time >30 min and temperature >475 °C). They have used the Delplot technique by Bhore et al. [5] for the explanation of reaction pathways. Delplot analysis is a useful tool to analyze reaction pathways in a complex reaction network system such as cracking of residual feedstocks.

1.2. Cracking behavior

The studies reported reveal that the resids with high asphaltene content are more reactive than resids with low asphaltene contents [6]. It has also been reported that the feedstocks with more saturates yield comparatively more gas oil fractions than gases and gasoline whereas more naphthenic/aromatic feedstock yield more light fractions, e.g., gases and gasoline [7] due to presence of small side chains attached to naphthenic/aromatic ring.

1.3. Lumping schemes

A number of lumped parameter models have been reported. Some studies are reported with one feed and one product lump [7–9], whereas numbers of lumps have been reported up to 16 [10]. The criteria for lumping have been based upon statistical information [11,12], characteristic information [13] or pseudo components [6,14,15]. The pseudo component lumping schemes suggested by Del Bianco et al. [14] does not describe distillate, as separated lumps of gasoline and gas oil fractions, and therefore, it cannot be applied for the design and optimization of a mild thermal cracking process to maximize distillates. The coke lump has been considered, which makes it suitable for describing more severe thermal cracking.

A review of studies done so far reveals that the models available are either highly structural information based, or high severity process models in which the coke is also taken as a lump. The detailed study of thermal cracking in terms of lumps of distillates is still not well understood due to lack of detailed analysis of distillate fractions. Based on the higher demand of distillate oils and decreasing use of residual fuel oils, thermal cracking process for residual feedstock needs development in terms of production of distillates.

The present study is focused on the development of a five lump model for low severity thermal cracking. The lumps considered are vacuum residue feedstock (F) and four cracked products namely Gas (-C_5), gasoline (IBP-150 °C), light gas oil (LGO) (150–350 °C) and vacuum gas oil (VGO) (350–500 °C). A ten kinetic parameter model was hypothesized. After a rigorous mathematical and theoretical analysis number of kinetic parameters was reduced to seven. The data used were obtained in the laboratory by thermal cracking of four different vacuum residues of Indian and Middle East origin in a stainless steel batch reactor of 400 ml capacity.

2. Experimental procedure

Experiments were conducted in a 400 ml stainless steel batch reactor. A common inlet/outlet was provided for charging and evacuating the reactor. Provisions were made to measure liquid and vapor temperatures separately, as well as pressure. A needle valve was provided for the pressure regulation and gas discharge during and after the reaction. The reactor was charged with 120 g of vacuum residue (feed) and pressurized with nitrogen to obtain a pressure of 12 kg/cm^2 (g) at reaction temperature. The heat required for the reaction was provided by a salt bath containing a eutectic mixture of $NaNO_3$, KNO_3 and $NaNO_2$ with its composition as 7, 53 and 40 wt.%, respectively.

The measurement of reaction time (residence time) was made from the moment when the liquid temperature reached the desired reaction temperature. Time for attaining the reaction temperature from the instant it is dipped into the salt bath, was found to be about 60–90 s for conducted experi-

Table 1
Feed characteristic

Serial numbers	Characteristic parameter	Feed			
		MVBF	HRA	BHSR	NGSR
(1)	Merit number	2.50	2.00	–	–
(2)	*n*-C_5 insolubles (wt.%)	13.19	26.92	7.25	11.24
(3)	*n*-C_7 insolubles (wt.%)	8.90	12.70	4.46	2.11
(4)	Asphaltenes (wt.%)	7.72	10.15	3.03	1.85
(5)	Pour point (°C)	+39	+72	+69	+48
(6)	Metals (elements, mg/L)				
	V, vanadium	29.30	95.75	3.40	43.00
	Ni, nickel	36.55	46.30	24.95	167.15
	Fe, iron	22.90	30.80	8.30	19.30
(7)	Density D_4^{15}	1.0176	1.0542	0.9636	0.9887
(8)	Kinetic viscosity, cSt at 100 °C	526.50	8217.30	91.30	1522.00
(9)	Kinetic viscosity, cSt at 135 °C	102.30	690.70	24.40	288.83
(10)	Sulfur (wt.%)	4.29	4.93	0.45	0.28
(11)	CCR (wt.%)	19.80	25.70	12.80	15.36
(12)	C/H ratio	7.50	7.78	5.58	7.85
(13)	Molecular weight	871.2	1078.8	793.5	–
(14)	Hydrocarbon type				
	Saturates	14.76	5.63	32.89	10.30
	Aromatics, naphthenic	67.85	68.07	59.82	58.71
	Polar	6.40	11.86	4.23	29.20
	n-C_7 insolubles	10.47	13.69	4.46	2.11

ments. The condensable hydrocarbon vapours were separated by passing the outlet gases from reactor through a condenser assembly. A gas meter was used to measure the volume of outlet gases.

The cracking of the feedstock may actually start during the period of preheating, i.e., even before the measurement of residence time is started. Therefore, the conversions of all the four feedstocks were determined during the time interval, required for attaining the desired reaction temperature, by conducting blank experiments, by heating a measured quantity of the feedstock up to the reaction temperature and measuring the conversion. The results of these blank experiments reveal the appreciable conversion only in the case of BHSR and MVBF feedstocks, within the temperature range of 410–430 °C. While estimating the kinetic parameters, these conversions were duly accounted for.

After the completion of the reaction time, the reactor was taken out and quenched in a water reservoir kept at room temperature. It was cooled down at a temperature near 100 °C and de-pressurized completely. The exit gas was collected and analyzed by gas chromatography for some representative runs, since the outlet gas composition does not vary significantly.

The liquid product from the reactor is quantified by weighing the reactor after drying and cleaning the outer surface. It contains unconverted vacuum residue and cracked products. Since the quantity of feedstock was too less to be precisely fractionated by distillation, it was analyzed by ASTM D-2887 (SIMDIST) procedure. Prior to analysis of the sample, the distillate fraction boiling up to 500 °C was separated out by atmospheric and vacuum distillation.

Detailed characteristics of the studied feedstocks have been listed in Table 1. The experimental results have been analyzed and described elsewhere [16] in detail.

3. Kinetic modelling of thermal cracking

It comprises of three subsections, selection of lumps, model development and the estimation of kinetic parameters. Analysis of results is described in the separate section.

3.1. Selection of lumps

Generally lumps may be chosen on the basis of certain easy to measure physical properties, e.g., boiling range, specific gravity. These lumps should have significance vis-à-vis the thermal cracking behaviour of the residue. A model with a large number of lumps is often computationally more expensive to solve. Therefore, it is always desirable to optimize the number of lumps to get maximum possible information about a process at the minimum computational cost.

In the present study, the feedstocks studied were vacuum residues (BHSR, NGSR), vacuum residues blended with oil fluxes (MVBF) and the asphalt from deasphalting process (HRA). The asphaltene contents of the feedstocks varied from 1.85 to 10.15% by weight. In order to avoid coke formation, the experiments were conducted at mild conditions. The cracked residue was separated into distillate (−500 °C) fractions and unconverted residue (+500 °C). As stated earlier, the distillate was analyzed using ASTM D2887 (SIMDIST)

procedure. The models available for such kind of feedstocks were at severe conditions, where coke formation was significant. Therefore, these models are not as such applicable for mild thermal cracking. Model suggested by Zhou et al. [15] considers six feedstock lumps, which requires a detailed feed characterization. In Del Bianco et al. [14] model, distillate was not analyzed further.

In order to explore the possibilities of heavy oil upgradation to generate distillate fuels and downstream feedstocks for secondary processes, e.g., FCC, lumps equivalent to gasoline fraction, light gas oil and vacuum gas oil seem to be more appropriate. Gas formed during the reaction constitutes another additional lump. Simulated distillation output yields percent distilled at various temperatures with cut range of every 1% distilled. Therefore, we have a flexibility to make the lumps (fractions) of practical interest for the development of a multi-lump kinetic model by using the experimental observations. Therefore, five lumps were considered on the similar lines to those suggested in the literature on the thermal cracking of short residues [14]. Four product lumps, namely gas, gasoline (IBP-150 °C), LGO (150–350 °C) and VGO (350–500 °C), and a feedstock (+500 °C) lump were chosen, based on boiling ranges.

3.2. Model development

In view of the above, a five lump model has been formulated as shown in Fig. 1. All the conversions were assumed to follow first-order reaction kinetics. The rate equations for the reaction network can be written as follows:

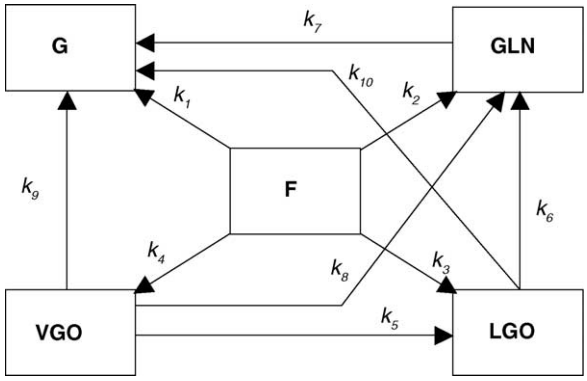

Fig. 1. Five lump model for thermal cracking. F: Feedstock (vacuum residue) +500°C, G: gas (-C_5), GLN: gasoline (IBP-150 °C), LGO: light gas oil (150–350 °C), VGO: vacuum gas oil (350–500 °C).

$$\frac{d[F]}{dt} = -(k_1 + k_2 + k_3 + k_4)[F] \quad (1)$$

$$\frac{d[\mathrm{VGO}]}{dt} = k_4[F] - (k_5 + k_8 + k_9)[\mathrm{VGO}] \quad (2)$$

$$\frac{d[\mathrm{LGO}]}{dt} = k_3[F] + k_5[\mathrm{VGO}] - (k_6 + k_{10})[\mathrm{LGO}] \quad (3)$$

$$\frac{d[\mathrm{GLN}]}{dt} = k_2[F] + k_6[\mathrm{LGO}] + k_8[\mathrm{VGO}] - k_7[\mathrm{GLN}] \quad (4)$$

$$\frac{d[G]}{dt} = k_1[F] + k_7[\mathrm{GLN}] + k_{10}[\mathrm{LGO}] + k_9[\mathrm{VGO}] \quad (5)$$

Initial conditions

At $t = 0$, $[F] = F_0$, $[\mathrm{VGO}] = [\mathrm{LGO}] = [\mathrm{GLN}] = [G] = 0$.

It is mentioned that the square brackets in the equations refer to the weight percent of the various fractions at time t. The above equations are homogeneous differential equations and can be easily solved with the above initial conditions. The solution of these equations results in following equations for various lumps in terms of F_0, i.e., initial weight of feedstock.

$$[F] = F_0 \exp(-K_A t) \quad (6)$$

$$[\mathrm{VGO}] = \frac{k_4 F_0}{K_B - K_A}[\exp(-K_A t) - \exp(-K_B t)] \quad (7)$$

$$[\mathrm{LGO}] = F_0[A\exp(-K_A t) - B\exp(-K_B t) + (B - A)\exp(-K_C t)] \quad (8)$$

$$[\mathrm{GLN}] = F_0\left[A_1\exp(-K_A t) - B_1\exp(-K_B t) + C_1\exp(-K_C t) + (B_1 - A_1 - C_1)\exp(-k_7 t)\right] \quad (9)$$

$$[\mathrm{GAS}] = F_0\left[\frac{1}{K_A}\left(k_1 + \frac{k_4 k_9}{(K_B - K_A)} + A_1 k_7 + A k_{10}\right)(1 - \exp(-K_A t)) - \frac{1}{K_B}\left(\frac{k_4 k_9}{K_B - K_A} + B_1 k_7 + B k_{10}\right) \times (1 - \exp(-K_B t)) + \frac{1}{K_C}((B - A)k_{10} + C_1 k_7)(1 - \exp(-K_C t)) + (B_1 - A_1 - C_1)(1 - \exp(-k_7 t))\right] \quad (10)$$

where

$$K_A = k_1 + k_2 + k_3 + k_4 \quad (11)$$

$$K_B = k_5 + k_8 + k_9 \quad (12)$$

$$K_C = k_6 + k_{10} \quad (13)$$

$$A = \frac{1}{K_C - K_A}\left(k_3 + \frac{k_4 k_5}{K_B - K_A}\right) \quad (14)$$

$$B = \left(\frac{k_4 k_5}{(K_B - K_A)(K_C - K_B)}\right) \quad (15)$$

$$A_1 = \left[k_2 + A\,k_6 + \frac{k_4 k_8}{K_B - K_A}\right]\frac{1}{k_7 - K_A} \quad (16)$$

$$B_1 = \left[B\,k_6 + \frac{k_4 k_8}{K_B - K_A}\right]\frac{1}{k_7 - K_B} \quad (17)$$

$$C_1 = \frac{(B - A)k_6}{k_7 - K_C} \quad (18)$$

3.3. Estimation of kinetic parameters

The differential evolution method (DEM) [17] was used for the estimation of parameters k_1 through k_{10}. It is an optimization technique from the family of genetic algorithms. It has been successfully tested for the design situations, where up to 60 parameters are required to be tuned. The advantages of DEM include its capability to find global optima, simple structure of algorithm, ease of use, fast speed and robustness, whereas gradient methods sometimes lead to local optimal solutions. Since it is based on the random search technique, it is not dependent on the initial guess. However, upper and lower bounds of values assumed by variables are to be specified. These were the reasons for our choice of this optimization method. For parameter estimation, sum of fractional error E_f, as given below, was minimized.

$$E_f = \sum_i \frac{|(Y_i^{exp} - Y_i^{pred})|}{Y_i^{pred}}$$

where Y_i^{exp} is the experimental value of the product yield and is theoretically calculated yield with the derived model Eqs. (6) through (10). Minimization of the sum of squares of error as well as percent error was also tried, but the minimization of E_f yielded the best results. Optimal governing parameters for DEM were selected on the basis of recommendations by Gämperle et al. [18].

4. Results and discussion

The kinetic parameters for the assumed model (Fig. 1) were estimated using experimental data for four feedstocks. The first hand estimate of the parameters revealed that the values of k_8–k_{10} were reasonably low in most of the cases. It indicates the least possibility of the reaction pathways by these routes. However, the values of kinetic parameters k_1–k_7 are significant. Rate constant k_8 assumes significant values at higher temperatures (>410 °C).

Flash calculations were performed with the final composition of reaction mixture using ASPEN plus flow sheet simulation software. Chao-Seader property option set was used in the simulation, which is a built in property option set in ASPEN and is most suitable for a hydrocarbon system at medium pressure. The simulation results revealed that the gasoline fraction would be mostly in vapour fraction, after formation. It may be therefore concluded that the reaction via path represented by the rate constant k_7 cannot be dominant, as gasoline fraction is very difficult to crack in vapor phase in the absence of a catalyst. The estimated values of rate constant k_7 are significant in few cases, but do not exhibit any regular trend either with temperature or time. Therefore, the consideration of pathways represented by kinetic constant k_7 would not be logical. Hence, k_7 was discarded from further analysis.

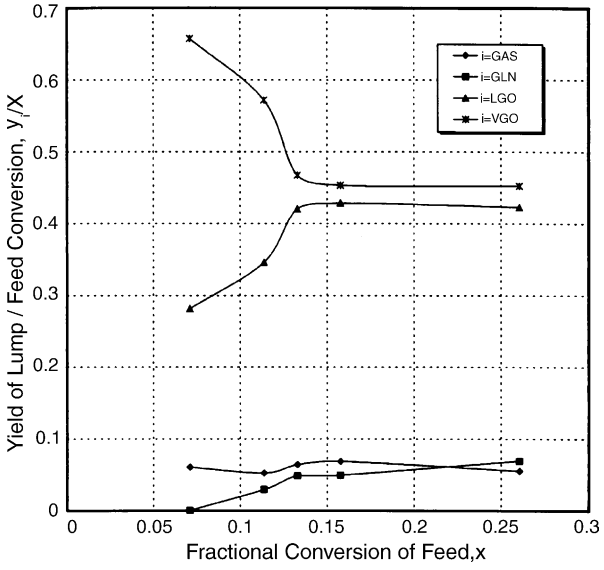

Fig. 2. First rank Delplots (feed: MVBF; T = 673 K).

A critical analysis of the selectivity of four product lumps for studied feedstocks with the temperature at different residence times revealed that the gas, gasoline and LGO selectivity increases with the increase in reaction time as well as temperature, whereas selectivity of VGO decreases with the increase in reaction time and temperature. For instance, the selectivities for NGSR feedstock, the percent selectivity increases for gas from 6.68 to 9.09, for gasoline from 0.97 to 5.54 and for LGO from 30.02 to 44.69, but the percent selectivity of VGO decreases from 62.35 to 40.68 as the temperature increases from 400 to 430 °C, at constant residence time of 3 min. Similar trend has been observed for the other residence times and reaction temperatures. The decrease in

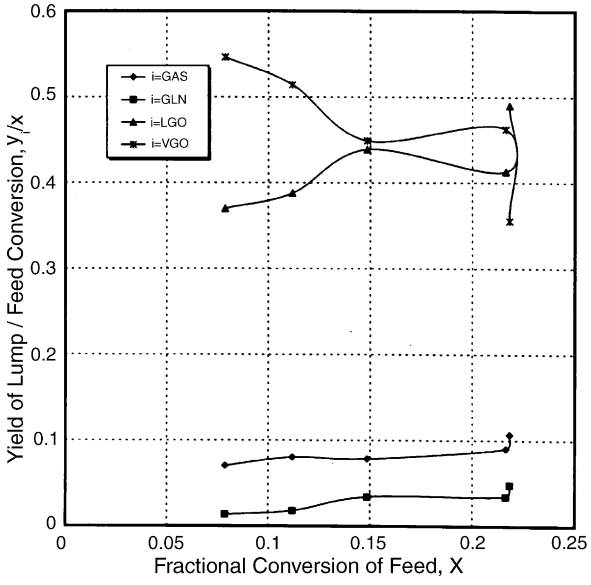

Fig. 3. First rank Delplots (feed: NGSR; T = 683 K).

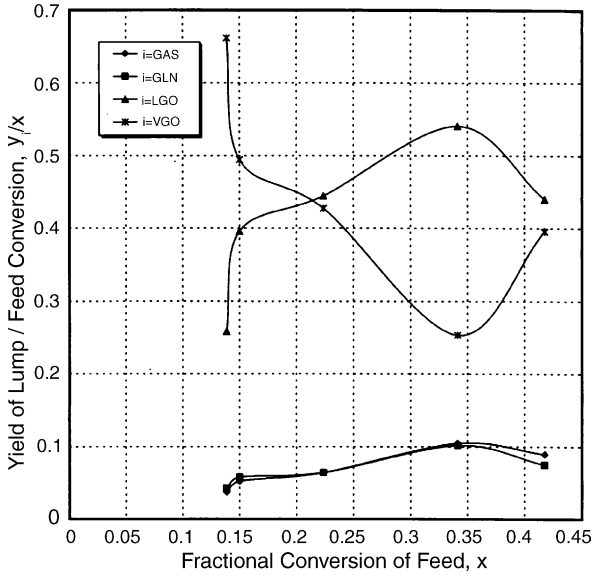

Fig. 4. First rank Delplots (feed: RHSB; $T = 693$ K).

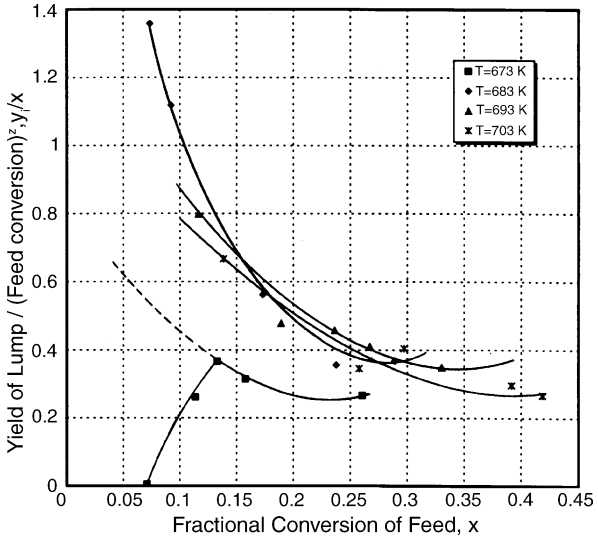

Fig. 6. Second rank Delplots for gasoline (feed: MVBF).

VGO fraction may be attributed to its significant secondary conversion to some of the other lumps.

4.1. Delplot analysis

In an attempt to establish a still better insight into the possible reaction network, Delpolt analysis [5] was done. Bhore et al. [5] have reported this technique by which reaction pathways can be established. The first rank Delplot is a curve between y_i/x and x, where x is overall conversion and y_i is yield of ith species. It allows us to separate the primary conversion in a reaction network from the secondary and tertiary conversions. If the intercept of first rank Delplot for a species i on y-axis is finite, it indicates that the species is being formed by primary conversion. A zero intercept at y-axis indicates that the species is not formed by primary conversion. However, it may be formed by secondary or tertiary reactions. Besides, reaction pathways for secondary or tertiary conversions can be established using higher rank Delplots or successive use of first rank Delplot. Second rank Delplot is defined as a plot between y_i/x^2 and x, third rank Delplot is between y_i/x^3 and x, and so on.

For the present study, first rank Delplots (Figs. 2–5) reveal that the conversion to gas and VGO lumps is essentially through primary reactions. The gasoline lump (GLN) appears to be formed by the secondary reaction, i.e., feed to VGO or LGO and then to GLN. At higher severities the conversion of feed to gasoline also shows finite intercept on y-axis in the first rank Delplot. Second rank Delplots reflect formation of GLN through tertiary conversion at lower temperature (Fig. 6). But at longer residence time as well as higher temperatures, the conversion does not appear taking place through tertiary reaction, i.e., first F to VGO, then VGO to

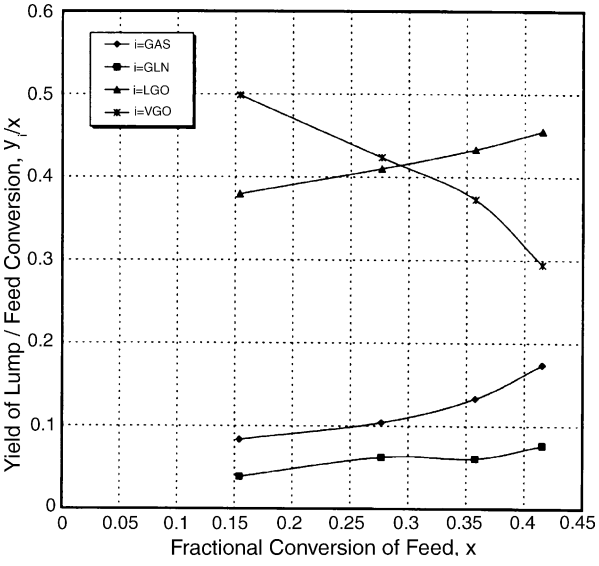

Fig. 5. First rank Delplots (feed: HRA; $T = 703$ K).

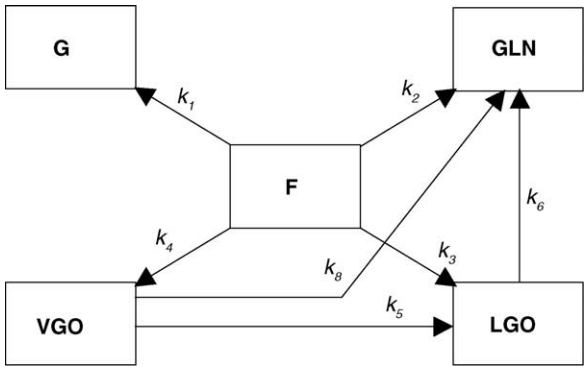

Fig. 7. Final five lump, seven parameter model for thermal cracking. F: Feedstock (vacuum residue) +500 °C, G: gas (-C_5) GLN: gasoline (IBP-150 °C), LGO: light gas oil (150–350 °C) VGO: vacuum gas oil (350–500 °C).

Table 2
Activation energies (kJ/mol) of proposed reaction network for thermal cracking (temperature range = 400–430 °C)

Rate constant min^{-1}	Activation energy (E, kJ/mol) and frequency factor (A_0, min)							
	NGSR		BHSR		MVBF		HR asphalt[a]	
	E	A_0	E	A_0	E	A_0	E	A_0
k_1	194.69	1.41E12	269.79	3.80E17	181.15	8.48E10	238.61	3.25E15
k_2	494.79	2.45E34	308.94	3.38E20	383.30	1.28E26	92.72[c]	1.05E04
k_3	202.52	2.32E13	234.54	5.50E15	225.85	1.28E15	64.07[c]	7.37E02
k_4	157.34	1.33E10	72.29[c]	5.22E03	139.90	4.64E08	179.56	6.68E11
$k_{5,8}$	258.07	2.05E18	412.50	7.80E29	84.20[c]	1.94E05	316.18	3.66E22
k_6	[b]		129.29[c]	7.66E07	[b]		[b]	

[a] The values are over a temperature range of 410–430 °C.
[b] Only one data point is available.
[c] In this temperature range, k remains approximately constant.

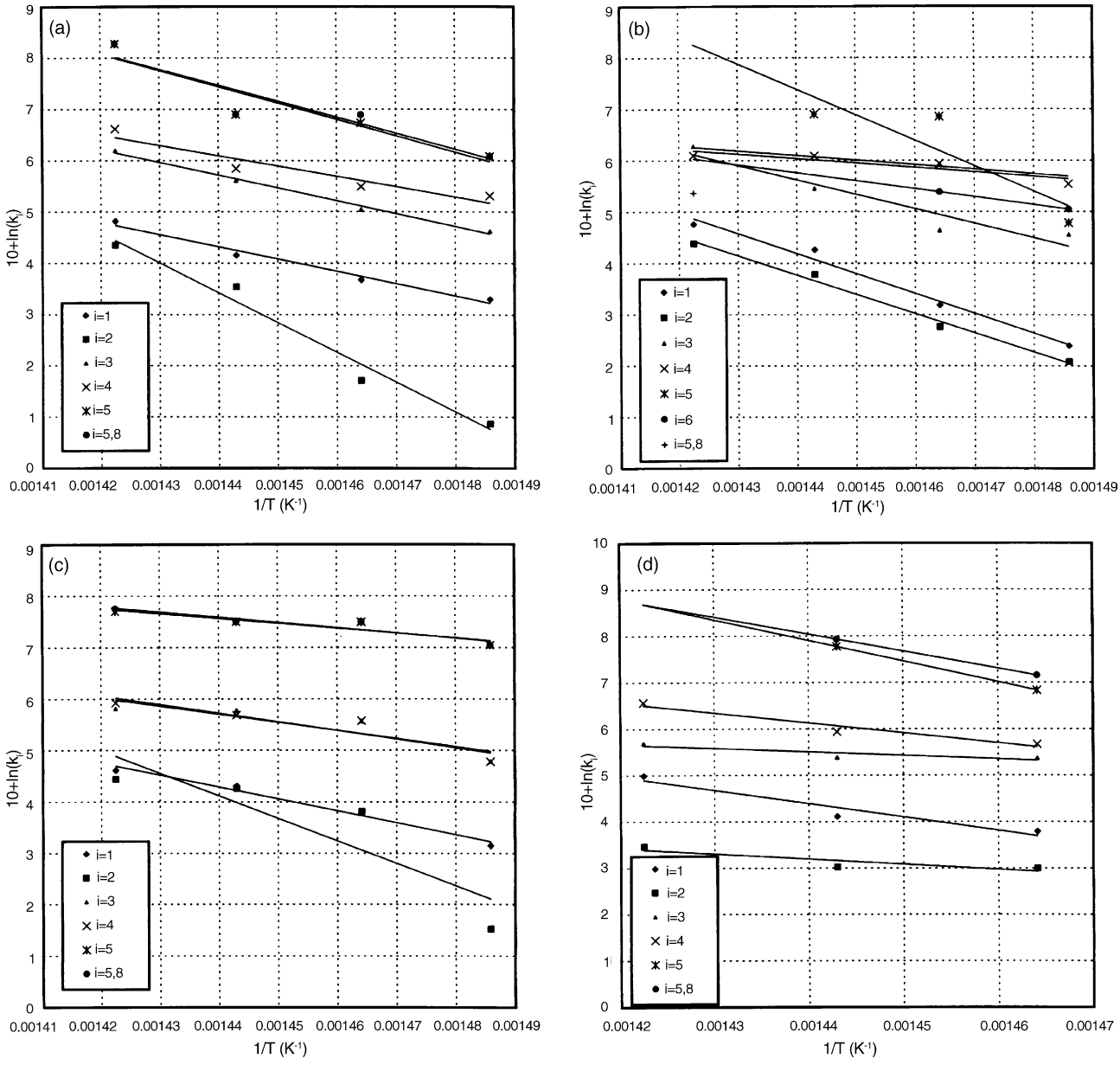

Fig. 8. (a) Arrhenius curves for reaction pathways, (feed: NGSR). (b) Arrhenius curves for reaction pathways, (feed: BHSR). (c) Arrhenius curves for reaction pathways (feed: MVBF). (d) Arrhenius curves for reaction pathways (feed: HRA).

LGO followed by LGO to gasoline (GLN). This behavior may be explained on the basis of calculated activation energies of various conversions reported later in the Table 2. The activation energy of the conversion from LGO to GLN fraction is small (129.29 kJ/mol in case of BHSR feedstock). In fact the kinetic constant k_6 is approximately constant in the range of our studied temperatures. Whereas, the activation energies for the conversion of feed to GLN (308 kJ/mol) and VGO to GLN ($k_{5,8}$ = 412 kJ/mol) are significant. Due to this reason, second rank Delplots seems to have near zero intercept at lower temperatures, which indicates tertiary formation of GLN, but at higher temperatures the intercept at *y*-axis becomes finite. It is also clear from the flash simulations by ASPEN plus, that at a temperature beyond 410 °C, liquid fraction of VGO and LGO gradually decreases, which results in the reduction of rate of cracking of these two fractions. It is also worthwhile to mention here that the thermal cracking normally occurs in liquid phase only.

4.2. Reduced parameter model

Based on the values of rate constants obtained by the parameter estimation and Delplot analysis, it is clearly indicated that the reactions governed by kinetic parameters k_7–k_{10} will not be dominant in the proposed reaction network. Among these parameters, k_8 assumes significant value at a temperature 430 °C. Therefore, the reaction pathways via k_7, k_9 and k_{10} may be dropped to develop a realistic model of the thermal cracking. On this basis a reduced parameter model has been evolved and is depicted in the Fig. 7. The parameter evaluation was repeated for this reduced model. It was observed that the value of k_8 is negligible at low severities and it assumes significant values at higher severities indicating the conversion of VGO to gasoline at these conditions. Further, it was also be noted that the values of remaining kinetic constants do not alter appreciably by dropping k_7, k_9 and k_{10} from the comprehensive model. The Arrhenius plots drawn for all the four feedstocks have been shown in Fig. 8a–d. The activation energies and frequency factors, for all the seven parameters have been computed and are given in Table 2.

4.3. Goodness of fit

The kinetic parameters successfully describe the reaction pathways hypothesized and evolved as shown in Fig. 7. Figs. 9–12 show the experimental and predicted values of yield from the model, plotted as yield versus residence time. Lines have been drawn to represent the predicted values, while experimental data have been shown by points. These curves show very good agreement between the experimental and predicted values. It is also evident from these curves that the data predictions using reduced seven parameter model (curves drawn by continuous lines) are more accurate as compared to those with ten kinetic parameter model (curves drawn by dashed lines). Table 3 shows the accuracy of predictions by proposed model. Nearly, 70% points are within

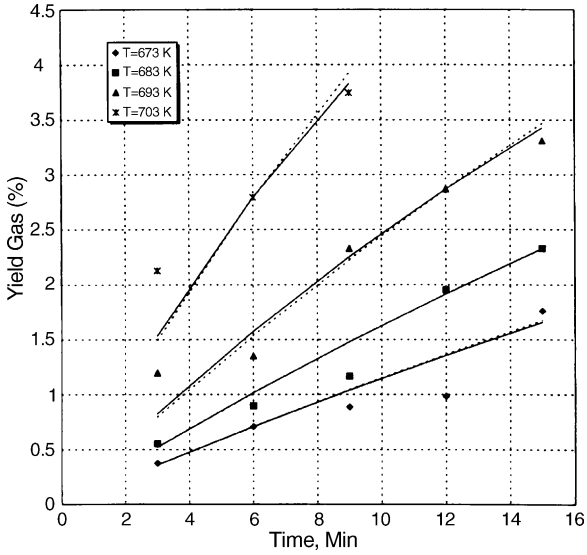

Fig. 9. Yield of gas with residence time (feed: NGSR) (continuous and dotted lines represent predicted values with seven and ten parameter models, respectively, while experimental data are shown by points.

±20% error. The error of this magnitude is acceptable for such complex reaction systems. It is therefore confirmed that the assumption of first-order kinetics predicts gas, gasoline and LGO fraction with very good accuracy. However, in the case of VGO conversion, the experimental yield patterns show deviation at higher temperatures and residence time. This is in agreement with the observations of Krishna et al. [9] that beyond a certain conversion level, the first-order kinetic behavior shows deviation.

In the analysis of the derived model, some questions are quite obvious. One may always wonder that the LGO, while being converted to GLN fraction, does not yield GAS. Simi-

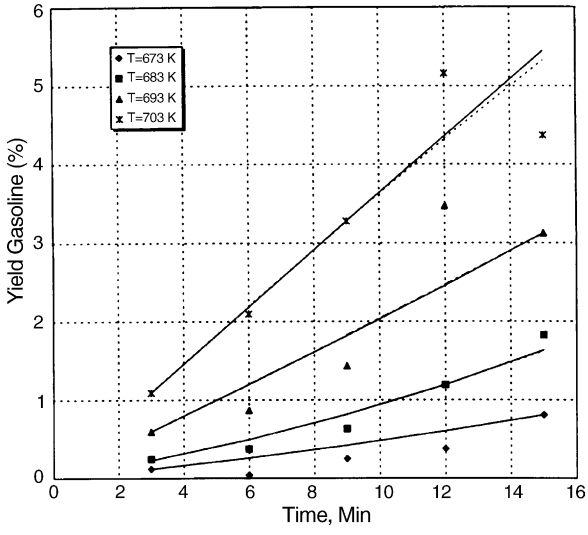

Fig. 10. Yield of gasoline with residence time (feed: BHSR) (continuous and dotted lines represent predicted values with seven and ten parameter models, respectively, while experimental data are shown by points).

Table 3
Error analysis of the predictions by five lump and seven parameter kinetic model

Feedstock	Percentage of predicted values within the error range of				Percentage of predicted values with error >30%
	10	15	20	30	
NGSR	58.33	68.02	73.61	84.72	15.28
BHSR	38.75	48.75	58.75	76.25	23.75
MVBF	53.75	63.75	71.25	83.75	16.25
HRA	53.85	61.54	69.23	80.76	19.24

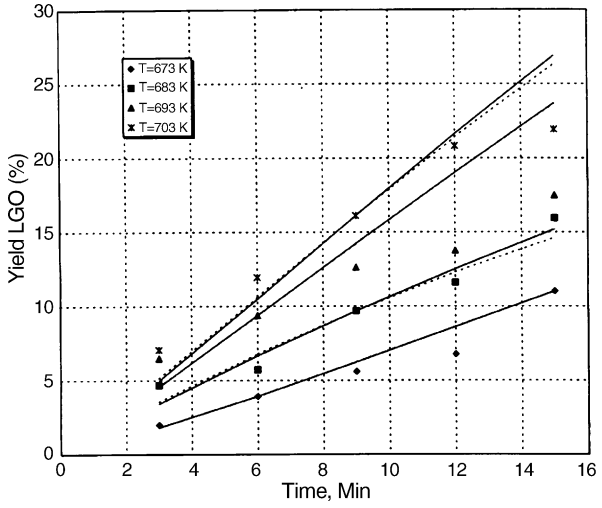

Fig. 11. Yield of LGO with residence time (feed: MVBF) (continuous and dotted lines represent predicted values with seven and ten parameter models, respectively, while experimental data are shown by points).

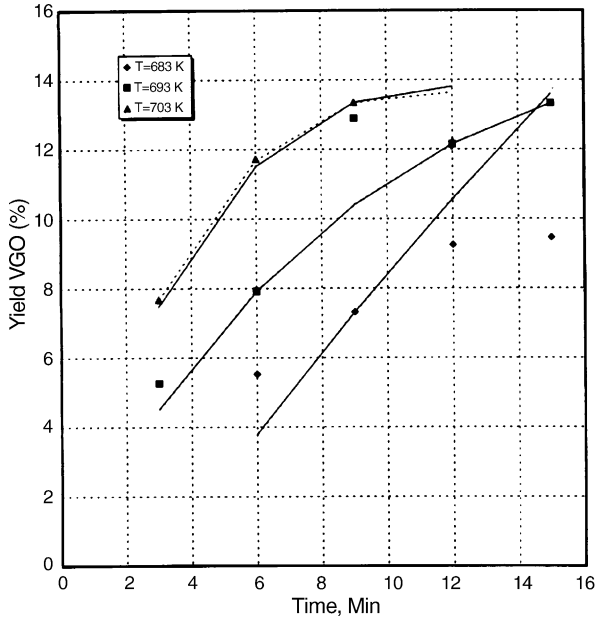

Fig. 12. Yield of VGO with residence time (feed: HRA) (continuous and dotted lines represent predicted values with seven and ten parameter models, respectively, while experimental data are shown by points).

larly the conversion of VGO to GLN and LGO shows up without any significant conversion to GAS. Although it sounds unusual, but it is possible that the conversion to gas via this route may be negligible, which does not appear in our analysis. The estimated kinetic parameters and activation energies are also markedly different for the studied feedstocks, for conversion to similar lumps. This may be due to the influence of the structural parameters, e.g., hydrocarbon types, length of paraffin chains attached to the aromatic and naphthenic compounds present in the feedstocks, etc. It is felt that a detailed structural analysis of the feedstocks as well as converted products is necessary to describe these variations precisely [16].

5. Conclusions

A five lump seven parameter kinetic model has been developed for the thermal cracking of residual feedstocks. The lumps were chosen on the basis of most value added products in a refinery. Delplot analysis [5] has been used to identify the reaction pathways. From this analysis, it has been concluded that the thermal cracking of vacuum residue feedstocks can be described by the developed five lump seven parameter kinetic model with greater accuracy within the operating temperature and pressure ranges for mild thermal cracking, e.g., visbreaking. The vapor liquid equilibrium in reaction system alters the linear kinetics of some of the lumps. But as such all the lumps seem to exhibit first-order kinetics.

References

[1] P.B. Crawford, W.A. Cunningham, Carbon formation in cat cracking, Pet. Refiner (1956 January) 169–173.
[2] M. Hus, Visbreaking process has strong revival, Oil Gas J. (April 13) (1981) 109–120.
[3] V.D. Singh, Visbreaking technology. Erdol und Kohle—Erdgas—Petrocheimie vereinigt mit Brennstoff-Chemie, Bd 39, Heft 1, 19–23, 1986.
[4] M.T. Martinez, A.M. Benito, M.A. Callejas, Thermal cracking of coal residues: kinetics of asphaltene decomposition, Fuel 6 (9) (1997) 871–877.
[5] N.A. Bhore, M.T. Klein, K.B. Bischoff, The Delplot technique: a new method for reaction pathway analysis, Ind. Eng. Chem. Res. 29 (1990) 313–316.

[6] M. Yasar, D.M. Trauth, M.T. Klein, Asphaltene and resid pyrolysis. Part 2. The effect of reaction environment on pathways and selectivities, Energy Fuels 15 (2001) 504–509.
[7] S. Di Carlo, B. Janis, Composition and visbreakability of petroleum residues, Chem. Eng. Sci. 47 (9–11) (1992) 2695–2700.
[8] H.H. Al Soufi, Z.F. Savaya, H.K. Mohammed, I.A. Al-Azawi, Thermal conversion (visbreaking) of heavy Iraqi residue, Fuel 67 (1988) 1714–1715.
[9] R. Krishna, Y.K. Kuchhal, G.S. Sarna, I.D. Singh, Visbreaking studies on Aghajari long residue, Fuel 67 (3) (1988) 379–383.
[10] R.M. Filho, M.F. Sugaya, A computer aided tool for heavy oil thermal cracking process simulation, Comput. Chem. Eng. 25 (2001) 683–692.
[11] M. Dente, Bozzano, Giulia, M. Rossi, Reactor and kinetic modelling of the visbreaking process, Proc. ICheaP1 (1993) 163–172.
[12] M. Dente, G. Bozzano, G. Bussani, A comprehensive program for visbreaking simulation: product amount and their properties prediction, Comput. Chem. Eng. (10) (1997) 1125–1134.
[13] J. Castellanos, J.L. Cano, R. Del Rosal, V.M. Briones, R.L. Mancilla, Kinetic model predicts visbreaker yields, Oil Gas J. 89 (11) (1991) 76–82.
[14] A. Del Bianco, G. Garuti, C. Pirovano, R. Russo, Thermal cracking of petroleum residues. Part 1. Kinetic analysis of the reaction, Fuel 74 (5) (1993) 756–760.
[15] S.L. Zhou, S.Z. Zhen, M.B. Wen, C.L. Lieh, C.K. Qia, Research study on dynamic model of complex reaction of vacuum residual oil, (translated from Chinese), ACTA Petrolei Sinica (Pet. Process. Sect.) 15 (2) (1999) 73–78.
[16] J. Singh, Thermal cracking of petroleum feedstocks: kinetics and process modelling studies, Ph.D. Thesis, Indian Institute of Technology Roorkee, Roorkee, India, 2004.
[17] R. Storn, K. Price, Differential evolution—a simple and efficient heuristic strategy for global optimization over continuous spaces, J. Global Optimization 11 (1997) 341–359, Dordrecht.
[18] Gämperle, R., Sibylle, D. Muller, Koumoutsakos, P., A parameter study for differential evolution, www.icos.ethz.ch/research/wseas02.pdf.